The angular dependence of Néel wall resistance by magnetotransport in the centipedelike Permalloy structures

T. Y. Chung and S. Y. Hsu

Citation: Journal of Applied Physics **105**, 07D123 (2009); doi: 10.1063/1.3068629
View online: http://dx.doi.org/10.1063/1.3068629
View Table of Contents: http://scitation.aip.org/content/aip/journal/jap/105/7?ver=pdfcov
Published by the AIP Publishing

The angular dependence of Néel wall resistance by magnetotransport in the centipedelike Permalloy structures

T. Y. Chung[a] and S. Y. Hsu
Institute of Electrophysics, National Chiao Tung University, Hsinchu 300, Taiwan

(Presented 11 November 2008; received 17 September 2008; accepted 8 November 2008; published online 27 February 2009)

The angular dependence of Néel wall resistance has been studied by measuring the in-plane magnetoresistances (MRs) of the centipedelike Permalloy (Py) structure, which consists of a central wire with numerous orthogonally bisecting finger wires. All Py wires were designed to have a single domain structure at remanence and high anisotropy by the geometric control. The remanent domain at the junction between the central and finger wires is determined by the anisotropy constants of both wires and hence, variable angles of Néel wall can be achieved. Using a simple resistance-in-series model in corporation with the anisotropic MR effect, the analyses of the longitudinal and transverse MRs of the centipedelike structure give the domain wall resistance. Our results show that the Néel wall resistance is about milliohm and decreases with decreasing the relative angle between two domains. © *2009 American Institute of Physics*.
[DOI: 10.1063/1.3068629]

The dynamic behavior of domain wall (DW) has been studied intensively in recent years. In addition to its fundamental interest, it is a potential candidate for the next generation of magnetic memory.[1] A detailed knowledge of the contribution to the resistivity when conduction electrons pass through DW has important consequences in the understanding of dynamic behavior.

In general cases, the contribution of DW scattering to the magnetoresistance (MR) is concealed by conventional sources of low temperature MR such as anisotropic magnetoresistance (AMR) and Lorentz MR in a ferromagnetic system. In order to isolate the domain wall resistance (DWR), it is necessary to create artificial domain walls using a unique pattern such as adding a neck to the wires,[2] designing zigzag structures,[3] forming a striped domain by thickness modulation[4] or exchange biases,[5] and implementing an elaborate magnetic field history process.[6] Although the DWRs were observed in various systems, both positive[2–8] and negative[9] values were reported with their theoretical justifications.[10–12] Up to now, the sign and the magnitude of the DWR and the fundamental mechanism of DW scattering are still controversial.

Most investigations to this subject focus on either 90° or 180° DW structures, regardless of the Néel or Bloch wall. In this work, we have fabricated the centipedelike Permalloy (Py) structures to obtain a series of Néel wall with various relative angles between two domains. The angular dependence of Néel wall resistance is explored by analyzing the longitudinal and transverse MRs based on a simple resistance-in-series model.

The centipedelike Py structures in submicron scale were made using standard e-beam lithography, thermal evaporation, and lift-off techniques. As shown in Fig. 1, each structure consists of a central wire and several finger wires that bisect orthogonally the central wire. All wires have a thickness of 30 nm. The central wire is 60 μm long and 1 μm wide (W). All finger wires are 20 μm long but have various widths (w: 0.3, 0.4, 0.5, 0.8, 1, and 1.5 μm). For a constant finger width, we made several series of structures with either different pitch l between the neighboring fingers ($1w \leq l \leq 10w$) or number of fingers n systematically. Figure 1 is a scanning electron microscopy (SEM) picture of one typical sample with $w=l=0.5$ μm. Brighter stripes are the nonmagnetic Au contacts serving as the voltage leads for MR measurements.

Magnetic domain structure and magnetotransport measurements were performed. The former was obtained using a magnetic force microscope (Digital Instruments Nanoscope IIIa) in tapping/lift mode. In this mode the topography and magnetic contrast can be well separated. The magnetic configuration was then imaged by monitoring the frequency or phase shift of the cantilever at a lift height of 100 nm. The latter was performed at the center of an in-plane electromagnet in a pumped ^{4}He cryostat. To avoid thermal fluctuation,

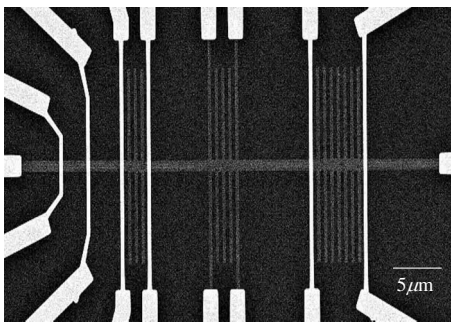

FIG. 1. A SEM image of one typical sample. The gray area is Py and the brighter wires are Au. The central wire of Py is 60 μm long and 1 μm wide. Two structures of three and seven finger wires are arranged with $w=l=0.5$ μm. The other structure at the center is arranged for the PHE measurement.

[a]Electronic mail: siky.ep86@nctu.edu.tw.

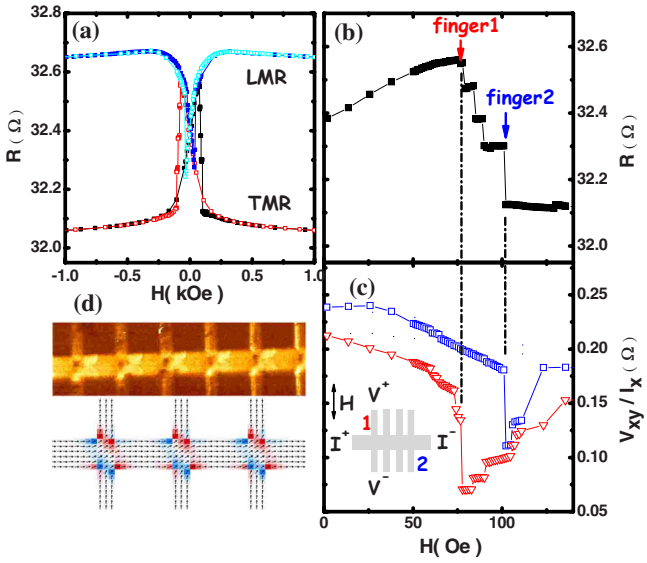

FIG. 2. (Color online) (a) LMR and TMR of one sample with $w=l=0.8$ μm and $n=4$. (b) An enlargement of the TMR at low field. Magnetic field is applied from 0 to 170 Oe. (c) Field dependence of transverse voltages V_{xy} divided by the current I_x for two fingers labeled as 1 and 2 in the scheme. (d) (Top) Remanent MFM image of one sample with $w=0.5$ μm and $l=1.5$ μm. (Bottom) Micromagnetic simulation of the magnetization configuration of the similar sample with the reduced dimensions by a factor of 0.1.

the MR was carried out at 10 K using a lock-in method. In this study, the driving current of less than 0.1 mA always flows along the axis of the central wire. The magnetic field is applied either along the current for longitudinal magnetoresistance (LMR) or normal to the current for transverse magnetoresistance (TMR).

The magnetic configuration in the polycrystalline magnetic wire is dominated by the aspect ratio as a result of shape anisotropy. The uniaxial anisotropy constant (K_u) can be quantified by the fit of TMR to the Stoner–Wohlfarth model. Our previous studies show that the remanent magnetic configuration is a single domain and K_u decreases from 10.5 to 1.3×10^5 ergs/cm^3 for a 20 μm long Py wire with width from 0.1 to 2 μm.[13] These values are much larger than the magnetocrystalline anisotropic energy density by two orders of magnitude due to shape anisotropy. In our centipedelike structures, the moment of the central wire preferably lies parallel with the axis of the central wire, while those of the finger wires preferably lie perpendicularly.

LMR and TMR of one structure with four fingers are plotted in Fig. 2(a). The LMR is saturated at 1 kOe and slightly decreases as the magnetic field approaches zero due to the coherent rotation of finger wires. When the field sweeps to the opposite direction and about 35 Oe, the reversal is completed via a single jump, which is the switching characteristics of the central wire. The TMR has the lowest resistance at saturated field of 1 kOe. When the field is reduced to zero, the magnetization of the pitch coherently rotates to the axis of the central wire, while the magnetization of the fingers remains. When the field sweeps to the opposite direction in the range between 77 and 101 Oe, the MR curve exhibits clearly four successive plateaus, a staircase. Figure 2(b) is the magnification of TMR shown in Fig. 2(a). The number of steps is the same as the number of fingers. This is confirmed by a systematic investigation in structures, which have the same geometries of both wires but different number of fingers ($3\leq N\leq 40$). The abrupt resistance drop is ascribed to the switching of each finger wire. After the step sequence, all magnetizations almost lie along the field direction and the resistance smoothly back to the saturation value.

It is important to note that the resistance at remanence is a constant despite of different field scanning processes. As shown in Fig. 2(a), both LMR and TMR have the same value at $H=0$. As described in the last paragraph, we believe that there is a very stable remanent magnetic configuration that the moment of the pitch is along the axis of the central wire and the moment of the finger is perpendicular to the axis of the central wire. As to the junction, there are orthogonal moments at its four corners resulting in a tilted moment of the junction.

In order to obtain the tilted angle of the moments at the junction, the transverse voltage V_{xy} across the junction via the orthogonal finger in the presence of the in-plane magnetic field was measured. The measurement is the so-called planar Hall effect (PHE), which arises from the anisotropy of spin-orbital scattering in magnetic materials. V_{xy} is sensitive to the angle θ between the current density J and magnetization M.[14] Here, the magnetic field is along the axis of fingers (the y-axis). As shown in the inset in Fig. 2(c), the abrupt drops in V_{xy} of fingers 1 and 2 correspond to the dramatic rotations of moments at the junctions 1 and 2 in the coercive fields, 77 and 101 Oe, respectively. Both fields of the drops are the same as the first and last steps in the TMR of one centipedelike structure that consists of both fingers indicating the sequentially one-by-one moment switching of fingers. Furthermore, the sin 2θ dependence of V_{xy} allows us to estimate the tiled angle of moment at the junction for a series of fingers with various widths. The values obtained from PHE are very close to $\tan^{-1}(K_u^{\text{finger}}/K_u^{\text{central}})$ within an uncertainty of 3°. K_u^{finger} and K_u^{central} are the anisotropy constants of the finger and central wires, respectively. Therefore, remanent moment direction at the junction is fairly determined by the shape anisotropies of the pair of orthogonal intersecting wires. Here, the tilted angles in this study range from 40° to 80° with decreasing the finger width. Figure 2(d) is a remanent magnetic force microscopy (MFM) image for one segment of a centipedelike structure. The deviation in contrast of magnetic moments at each junction shows a regular pattern as opposed to showing no contrast at other position in the wires. The image can be roughly confirmed by a micromagnetic simulation using object oriented micromagnetic framework[15] [also see Fig. 2(d)].

For our centipedelike structures, a central wire orthogonally bisects n of individual finger wires as shown in the inset in Fig. 3. The whole structure can be divided to n junctions and $n+1$ central wire pitches. Each junction is connected to two central wire pitches. At remanence, the moment of the central wire lies preferably along the wire axis but the moment at the junction tilts due to finger wire. Hence, a Néel domain wall is present between the junction (↗ domain) and pitch (→ domain).

Although the response of moment distribution during the

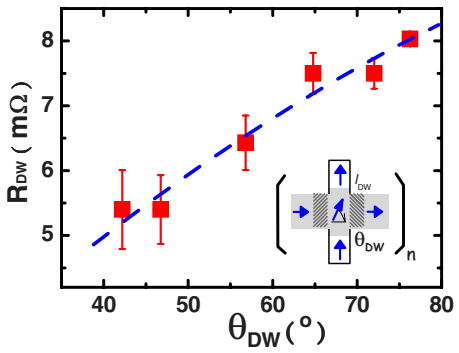

FIG. 3. (Color online) The angular dependence of the intrinsic DWR. The dashed line is a guide to the eye. The moment configuration of one segment of one typical sample is sketched in the inset.

field reversal process is quite complicated, the moment distributions at remanence and saturation field can easily be figured out. Upon these situations, we develop a resistance-in-series model to analyze the DWR. In this model, the MR is composed of the resistances contributed from these three regions and is written as

$$R(\vec{H}) = \frac{(n+1)l}{W} R_{\text{pitch}}(\vec{H}) + \frac{nw}{\alpha W} R_{\text{junction}}(\vec{H}) + 2n\left[R_{\text{DW}} - \frac{l_{\text{DW}}}{W} R_{\text{pitch}}(\vec{H}) + R_{\text{DW}}^{\text{AMR}} \right]. \quad (1)$$

Here α is the current distribution factor, which involves the influence of the nonuniform current density at the junction due to both open ends of a finger wire. R_{pitch} and R_{junction} are the sheet resistances of the pitch and junction, respectively. At the saturation field (>1 kOe), all moments lie along the magnetic field and the domain wall is absent. Only the first two terms contribute the whole resistance with that $R_{\text{pitch}} = R_{\text{junction}}$. The last term is a correction under the consideration of DWs ($H < H_{\text{sat}}$). Linear dependences of saturated LMR and TMR on both l and n give $R_{\text{pitch}}(\vec{H})$, $R_{\text{junction}}(\vec{H})$, and α.

At remanence ($H=0$), the moments at the junction tile at an angle θ_{DW} while those at most area of pitch lie along the axis of the central wire. The domain wall of length l_{DW} is created at both ends of each pitch. For the structure, there are $2n$ of domain wall and correspondingly, extra contribution of domain wall resistance, $2nR_{\text{DW}}$, is expected. Since moments of each domain wall rotate smoothly from angle θ_{DW} to zero relative to the axis of the central wire as shown in the inset in Fig. 3, original resistance of the region included in the first term of Eq. (1) should be deleted and additional AMR resistance should be taken into account. The domain wall width study in T-shaped Py structures by Haug *et al.*[16] gives the rough estimate of l_{DW}. The domain wall profile is assumed as a hyperbolic tangent function based on spin-polarized SEM studies in H shaped Py structures by Jubert *et al.*[17] and hence, $R_{\text{DW}}^{\text{AMR}}$ can be estimated for a given θ_{DW}. A systematic fit of remanent resistance to Eq. (1) give the self-consistent quantities of R_{DW}. Figure 3 demonstrates the angular dependence of R_{DW}. DWRs are positive and increase with increasing θ_{DW} from 42° to 76°.

One explanation for the positive DWRs is the mistracking effect[10,11] that DWR results from the scattering between the polarized conduction electrons with the localized magnetic moments and will be enhanced by the large spatial variation in magnetic moments in a DW.[11] Here, l_{DW} increases monotonically from 120 to 220 nm when θ_{DW} is changed from 76° to 42° implying a monotonic change in spatial variation in magnetic moments in a DW. Therefore, the result that DWR increases with increasing θ_{DW} can be attributed to the mistracking effect. For large θ_{DW}, the DWMR is about 0.75% close to the theoretical expectation by Levy and Zhang.[9]

The artificial Néel walls were created in the centipede-like Py structures. Measurements of LMR and TMR reveal information of their magnetic reversals. Due to the shape anisotropy, there is a stable periodic domain configuration of alternating pitch and junction. The tilted angle of moment at the junction is determined by anisotropy constants of both wires and is verified by the PHE measurement. A model of resistance-in-series is developed to analyze both MRs and the intrinsic DWR can be obtained. We find that DWR is positive and decreases with decreasing the angle. The result is indeed consistent with the prediction by consideration of the spin-mistracking effect.

MFM images were taken in the nanostructure laboratory of Dr. J. C. Wu. This work was supported by the NSC of Taiwan grant under Project No. NSC96-2112-M-009-030-MY3 and MOE ATU program.

[1]S. S. P. Parkin, M. Hayashi, and L. Thomas, Science **320**, 190 (2008).
[2]S. Lepadatu and Y. B. Xu, Phys. Rev. Lett. **92**, 127201 (2004).
[3]T. Taniyama, I. Nalatani, T. Namikawa, and Y. Yamazaki, Phys. Rev. Lett. **82**, 2780 (1999).
[4]W. L. Lee, F. Q. Zhu, and C. L. Chien, Appl. Phys. Lett. **88**, 122503 (2006).
[5]D. Buntinx, S. Brems, A. Volodin, K. Temst, and C. V. Haesendonck, Phys. Rev. Lett. **94**, 017204 (2005).
[6]U. Ebels, A. Radulescu, Y. Henry, L. Piraux, and K. Ounadjela, Phys. Rev. Lett. **84**, 983 (2000).
[7]R. Danneau, P. Warin, J. P. Attané, I. Petej, C. Beigné, C. Fermon, O. Klein, A. Marty, F. Ott, Y. Samson, and M. Viret, Phys. Rev. Lett. **88**, 157201 (2002).
[8]C. Hassel, M. Brands, F. Y. Lo, A. D. Wieck, and G. Dumpich, Phys. Rev. Lett. **97**, 226805 (2006).
[9]U. Ruediger, J. Yu, S. Zhang, A. D. Kent, and S. S. P. Parkin, Phys. Rev. Lett. **80**, 5639 (1998).
[10]P. M. Levy and S. Zhang, Phys. Rev. Lett. **79**, 5110 (1997).
[11]J. F. Gregg, W. Allen, K. Ounadjela, M. Viret, M. Hehn, S. M. Thompson, and J. M. D. Coey, Phys. Rev. Lett. **77**, 1580 (1996).
[12]G. Tatara and H. Fukuyama, Phys. Rev. Lett. **78**, 3773 (1997).
[13]T. Y. Chung and S. Y. Hsu (unpublished).
[14]H. Sato, R. Hanada, H. Sugawara, Y. Aoki, T. Ono, H. Miyajima, and T. Shinjo, Phys. Rev. B **61**, 3227 (2000).
[15]This code to calculate the magnetization configuration is described on http://math.nist.gov/oommf.
[16]T. Haug, C. H. Back, J. Raabe, S. Heun, and A. Locatelli, Appl. Phys. Lett. **86**, 152503 (2005).
[17]P. O. Jubert, R. Allenspach, and A. Bischof, Phys. Rev. B **69**, 220410 (2004).